Myricetin Suppresses UVB-Induced Skin Cancer by Targeting Fyn

Sung Keun Jung,[1] Ki Won Lee,[2] Sanguine Byun,[1] Nam Joo Kang,[1,4] Sung Hwan Lim,[1] Yong-Seok Heo,[3] Ann M. Bode,[4] G. Tim Bowden,[5] Hyong Joo Lee,[1] and Zigang Dong[4]

[1]Department of Agricultural Biotechnology, Seoul National University; [2]Department of Bioscience and Biotechnology and [3]Department of Chemistry, Konkuk University, Seoul, Republic of Korea; [4]The Hormel Institute, University of Minnesota, Austin, Minnesota; and [5]University of Arizona Cancer Center, Tucson, Arizona

Abstract

Skin cancer is currently the most common type of human cancer in Americans. Myricetin, a naturally occurring phytochemical, has potent anticancer-promoting activity and contributes to the chemopreventive potential of several foods, including red wine. Here, we show that myricetin suppresses UVB-induced cyclooxygenase-2 (COX-2) expression in mouse skin epidermal JB6 P+ cells. The activation of activator protein-1 and nuclear factor-κB induced by UVB was dose-dependently inhibited by myricetin treatment. Western blot and kinase assay data revealed that myricetin inhibited Fyn kinase activity and subsequently attenuated UVB-induced phosphorylation of mitogen-activated protein kinases. Pull-down assays revealed that myricetin competitively bound with ATP to suppress Fyn kinase activity. Importantly, myricetin exerted similar inhibitory effects compared with 4-amino-5-(4-chloro-phenyl)-7-(*t*-butyl)pyrazolo[3,4-*d*]pyrimidine, a well-known pharmacologic inhibitor of Fyn. *In vivo* mouse skin data also revealed that myricetin inhibited Fyn kinase activity directly and subsequently attenuated UVB-induced COX-2 expression. Mouse skin tumorigenesis data clearly showed that pretreatment with myricetin significantly suppressed UVB-induced skin tumor incidence in a dose-dependent manner. Docking data suggest that myricetin is easily docked to the ATP-binding site of Fyn, which is located between the N and C lobes of the kinase domain. Overall, these results indicated that myricetin exerts potent chemopreventive activity mainly by targeting Fyn in skin carcinogenesis. [Cancer Res 2008;68(14):6021–30]

Introduction

Skin cancer is currently the most common type of human cancer in Americans, and its incidence is increasing at an astonishing rate (1). Epidemiologic evidence and molecular studies suggest that nonmelanoma skin cancer is related to excessive exposure to the UV radiation in sunlight (2, 3). UV is divided into three subtypes, each of which has distinct biological effects: UVA (320–400 nm), UVB (280–320 nm), and UVC (200–280 nm; ref. 4). Although UVC is blocked by stratospheric ozone, UVB and UVA reach the surface of the earth and cause DNA damage, erythema, sunburn, immunosuppression, and, eventually, skin cancer (1). UVA, the major component of UV irradiation to which humans are exposed, is carcinogenic and causes photoaging and wrinkling of the skin. UVB is recognized as a complete carcinogen with relevance to human skin cancer (5, 6). Therefore, targeting UVB-induced signaling and signal molecules might be an effective strategy for preventing skin tumorigenesis.

Cyclooxygenase (COX), a rate-limiting enzyme for the oxidative conversion of arachidonic acids to prostaglandins, has two main isoforms: COX-1 and COX-2. COX-1 is a constitutively expressed isoform, and COX-2 is an inducible isoform (7). In human and murine skin cells, COX-2 is up-regulated in response to acute and chronic UVB irradiation (8). Celecoxib, a COX-2 inhibitor, has been shown to inhibit tumor formation in several animal models, including mouse skin (9). Several studies have found that up-regulated COX-2 expression in skin epidermis is involved in the development of skin cancer (10). Thus, developing an agent that can suppress COX-2 expression could be a critical strategy for the chemoprevention of skin cancer. The Src family kinases (SFK) consist of nine highly similar tyrosine kinases, and increased SFK activity is related to cellular events, including differentiation, proliferation, migration, and survival (11); SFKs are found in a variety of epithelial tumors, including ulcerative colitis, colonic adenocarcinoma, mammary carcinoma, and murine cutaneous squamous cell carcinoma (12–15). Activation of Fyn, a nonreceptor tyrosine kinase and member of the Src family, plays a critical role in the development of skin cancer (16, 17). Interactions of Fyn with various signaling molecules regulate diverse biological functions, such as the progression of carcinogenesis (13, 18). Activated Fyn promotes oral cancer progression via Raf-extracellular signal-regulated kinase (ERK) and integrin β_6 signaling (19), and the Fyn tyrosine kinase is a downstream mediator of Rho/PKR2 function in keratinocyte cell-cell adhesion (20). Multiple lines of evidence have shown a relationship between Fyn and skin abnormalities. Mice expressing double mutated $fyn^{-/-}fak^{+/-}$ exerted abnormal thickness of the epidermis and hyperdifferentiation of keratinocytes (21). Fyn also mediated keratinocyte migration and squamous carcinoma invasion through the disruption of a6b4 integrin (22). Thus, Fyn may be a molecular target for chemoprevention of skin cancer.

In an increasing number of studies, many naturally occurring phytochemicals that are present in the human diet have been recommended as potential chemoprevention agents (23), but the search for novel natural agents and the determination of novel targets for chemoprevention is challenging. Myricetin (3,3′,4′,5,5′,7-hexahydroxyflavone; Fig. 1*A*) is one of the major flavonoids found in various foods, including onions, berries, and grapes, as well as red wine (24–26). Research data have shown that myricetin exerts antioxidant, antitumor, and antiinflammatory effects (23, 27). A recent study showed that myricetin strongly inhibited tumor promoter–induced neoplastic cell transformation by direct inhibition of mitogen-activated protein kinase (MAPK)/ERK kinase

Note: S. K. Jung and K. W. Lee contributed equally to this work.

Requests for reprints: Hyong Joo Lee, Department of Agricultural Biotechnology, Seoul National University, Seoul 151-742, Republic of Korea. Phone: 82-2-880-4860; Fax: 82-2-873-5095; E-mail: leehyjo@snu.ac.kr or Zigang Dong, Hormel Institute, University of Minnesota, 801 16th Avenue NE, Austin, MN 55912. Phone: 507-437-9600; Fax: 507-437-9606; E-mail: zgdong@hi.umn.edu.

doi:10.1158/0008-5472.CAN-08-0899

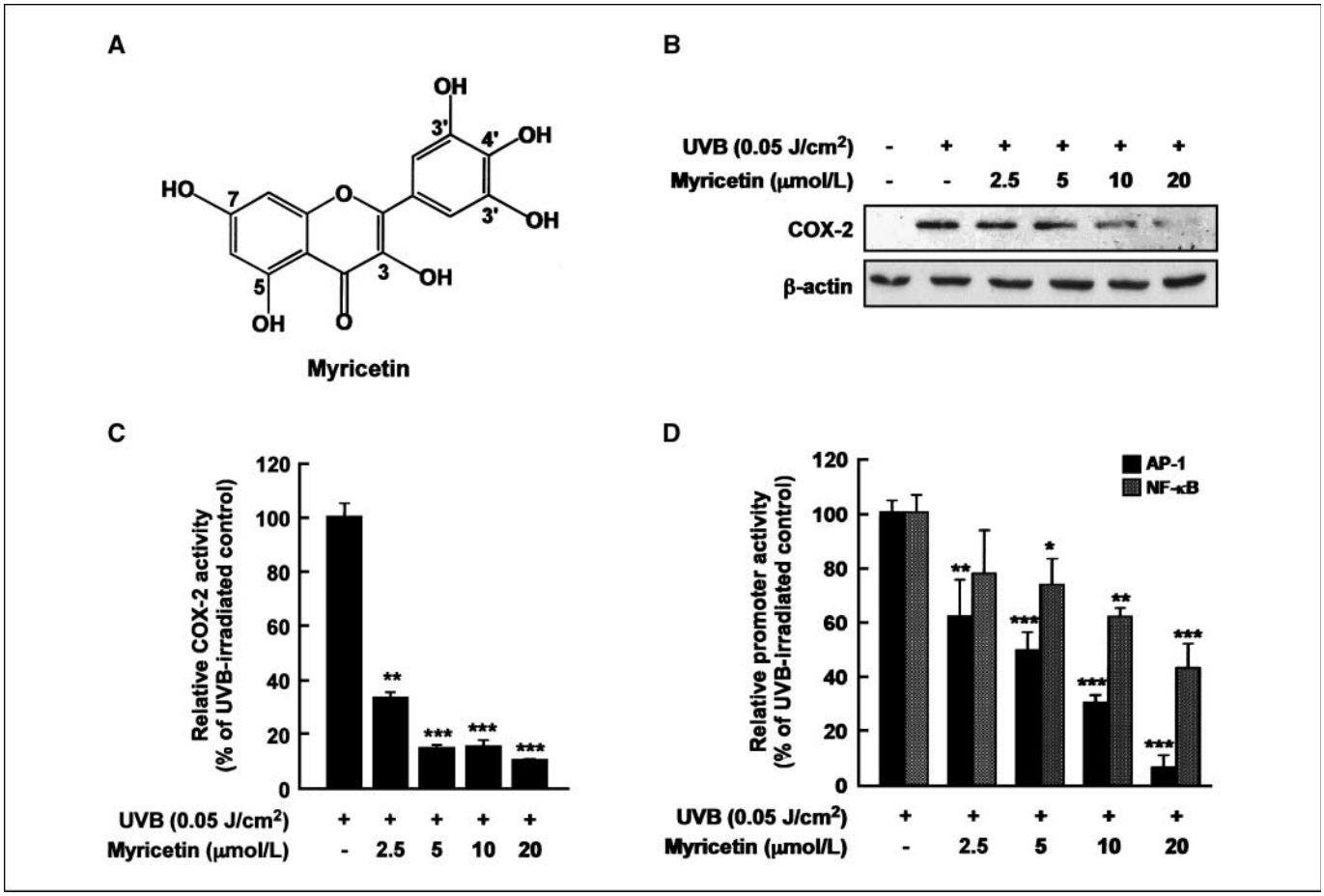

Figure 1. Effects of myricetin on UVB-induced COX-2 expression and AP-1 and NF-κB transactivation in JB6 P+ cells. *A,* chemical structure of myricetin with its numbering scheme. *B,* myricetin inhibits UVB-induced COX-2 expression in JB6 P+ cells. The levels of COX-2 and β-actin expression were determined by Western blot analysis using specific antibodies against the corresponding proteins as described in Materials and Methods. Data are representative of three independent experiments that gave similar results. *C* and *D,* myricetin inhibits UVB-induced COX-2 promoter activity and AP-1 and NF-κB transactivation. For the luciferase assay, JB6 cells stably transfected with an AP-1, NF-κB, or COX-2 luciferase reporter plasmid were cultured as described in Materials and Methods. The cells were starved in 0.1% FBS-MEM and then treated or not treated with myricetin at the indicated concentrations (0, 2.5, 5, 10, or 20 μmol/L) for 1 h before they were exposed to UVB (0.05 J/cm^2) and harvested 6 h later. Luciferase activity was assayed, and COX-2, AP-1, and NF-κB activity are expressed relative to cells treated with only UVB. Data are represented as the mean ± SD of AP-1, NF-κB, and COX-2 luciferase activity calculated from three independent experiments. *, **, and ***, significant differences at $P < 0.05$, $P < 0.01$, and $P < 0.001$, respectively, between groups treated with UVB and myricetin and the group treated with UVB alone.

(MEK) kinase activity (28). Moreover, its inhibitory effect was more potent than resveratrol, which is a well-known chemopreventive agent with anticancer effects (28). These accumulated data provide evidence that myricetin is a potent anticancer agent, but the underlying mechanism and target(s) in skin cancer are unclear. Here, we report that myricetin is an ATP-competitive inhibitor of Fyn and subsequently suppresses UVB-induced COX-2 expression in JB6 P+ mouse skin epidermal cells and in mouse dorsal skin. In a mouse skin tumorigenesis model, myricetin strongly suppressed UVB-induced incidence of mouse skin tumors.

Materials and Methods

Materials. Myricetin (>95% purity) and the antibody against β-actin were purchased from Sigma-Aldrich. Eagle's MEM, gentamicin, and L-glutamine were obtained from Life Technologies-Bethesda Research Laboratories. Fetal bovine serum (FBS) was purchased from Gemini Bio-Products, and 4-amino-5-(4-chloro-phenyl)-7-(*t*-butyl)pyrazolo[3,4-*d*]pyrimidine was obtained from Calbiochem. The antibody against COX-2 was purchased from Cayman. Antibodies to detect phosphorylated p38 (Tyr^{180}/Tyr^{182}), total p38, phosphorylated c-Jun NH_2 kinase (JNK; Thr^{183}/Tyr^{185}), total JNK, phosphorylated p90^{RSK} (Thr^{359}/Ser^{363}), total p90^{RSK}, phosphorylated MSK (Ser^{376}), total MSK, phosphorylated MEK1/2 (Ser$^{217/221}$), total MEK, phosphorylated Raf (Ser^{259}), and total Raf were purchased from Cell Signaling Biotechnology. Antibodies against phosphorylated Fyn (Thr^{12}), phosphorylated ERK1/2 (Thr^{202}/Tyr^{204}), and total ERK were obtained from Santa Cruz Biotechnology. The active Fyn protein and antibody against Fyn were obtained from Upstate Biotechnology. CNBr-sepharose 4B, glutathione-sepharose 4B, [γ-^{32}P]ATP, and the chemiluminescence detection kit were purchased from Amersham Pharmacia Biotech, and the protein assay kit was obtained from Bio-Rad Laboratories. G418 and the luciferase assay substrate were purchased from Promega. Eagle's MEM was from Invitrogen.

Cell culture. The JB6 P+ mouse epidermal cell line was cultured in 5% FBS-MEM, 2 mmol/L L-glutamine, and 25 μg/mL gentamicin in monolayers at 37°C in a 5% CO_2 incubator. The JB6 P+ mouse epidermal cell line was stably transfected with the activator protein-1 (AP-1), nuclear factor-κB (NF-κB), and COX-2 luciferase reporter plasmid and maintained in 5% FBS-MEM containing 200 μg/mL G418.

Animals. Female ICR mice and SKH-1 hairless mice (5 wk of age; mean body weight, 25 g) were purchased from the Institute of Laboratory Animal Resources at Seoul National University. Animals were acclimated for 1 wk before the study and had free access to food and water. The animals were

housed in climate-controlled quarters (24°C at 50% humidity) with a 12-h light/12-h dark cycle.

Luciferase assay for AP-1, NF-κB, and COX-2 transactivation. Confluent monolayers of JB6 P+ cells stably transfected with the AP-1, NF-κB, or COX-2 luciferase plasmid were harvested, and viable cells (8×10^3) were suspended in 100 μL of 5% FBS/MEM were added to each well of a 96-well plate. Plates were incubated at 37°C in a 5% CO_2 incubator. When cells reached 80% to 90% confluence, they were cultured in 0.1% FBS-MEM for another 24 h. The cells were treated 1 h with various concentrations of myricetin (0, 2.5, 5, 10, and 20 μmol/L) before exposure to UVB (0.05 J/cm^2) and were then incubated for 6 h. Cells were disrupted with 100 μL lysis buffer [0.1 mol/L potassium phosphate buffer (pH 7.8), 1% Triton X-100, 1 mmol/L DTT, and 2 mmol/L EDTA], and luciferase activity was measured using a luminometer (Luminoskan Ascent; Thermo Electron).

Western blot assays. For the *in vitro* Western blots, cells (1.5×10^6) were cultured in a 10-cm dish for 48 h and then starved in 0.1% FBS-MEM for 24 h to eliminate FBS activation of MAPKs. The cells were then treated with various concentrations of myricetin (0, 2.5, 5, 10, and 20 μmol/L) for 1 h and then irradiated with UVB (0.05 J/cm^2). The protein concentration was determined using a dye-binding protein assay kit (Bio-Rad Laboratories) as described by the manufacturer. Lysate protein (40 μg) was subjected to 10% SDS-PAGE and transferred to a polyvinylidene difluoride (PVDF) membrane (Amersham Pharmacia Biotech). After transfer, the membrane was incubated with the specific primary antibody at 4°C overnight. Protein bands were visualized by a chemiluminescence detection kit (Amersham Pharmacia Biotech) after hybridization with a horseradish peroxidase–conjugated secondary antibody. The relative amounts of proteins associated with specific antibodies were quantified using Scion Image (NIH).

For the *in vivo* Western blots, mice received topical application of myricetin (0, 5, 25, or 125 nmol) in 200 μL acetone on their shaved backs 1 h before UVB irradiation. To isolate protein from mouse skin, the dorsal skin of each mouse was excised and placed on ice. Any fat was removed, and the skin was placed in liquid nitrogen and immediately pulverized with a mortar and pestle. The pulverized skin was blended on ice with a homogenizer (IKA T10 basic; IKA Laboratory Equipment), and skin lysates were centrifuged at 12,000 rpm for 20 min. After the protein content was determined using the Bio-Rad protein assay kit, 100 μg of mouse skin extract was subjected to 10% SDS-PAGE and transferred to a PVDF membrane (Amersham Pharmacia Biotech). Membranes were processed, and proteins were analyzed as described above for the *in vitro* Western blot assay.

Fyn kinase assays. The *in vitro* kinase assays were performed in accordance with the instructions provided by Upstate Biotechnology. In brief, every reaction solution contained 20 μL of assay dilution buffer [20 mmol/L MOPS (pH 7.2), 25 mmol/L β-glycerol phosphate, 5 mmol/L EGTA, 1 mmol/L sodium orthovanadate, and 1 mmol/L DTT] and a magnesium-ATP cocktail buffer. For Fyn, 250 μmol/L of the Src substrate peptide were also included. A 2.5-μL aliquot was removed from the reaction mixture, which contained 2.5 μL of 250 μmol/L Src substrate and 10 μL diluted [γ-^{32}P]ATP solution and incubated at 30°C for 30 min, and then 15-μL aliquots were transferred onto p81 paper and washed thrice with 0.75% phosphoric acid for 5 min/wash and once with acetone for 5 min. The radioactive incorporation was determined using a scintillation counter. The effect of myricetin (0, 2.5, 5, 10, and 20 μmol/L) was evaluated by separately incubating each compound with the reaction mixtures at 30°C for 10 min. Each experiment was performed thrice.

For *ex vivo* Fyn immunoprecipitation and kinase assays, 500 μg of cell lysate protein was mixed with protein-A/G beads (20 μL) for 1 h at 4°C in advance. The mixture was centrifuged at 12,000 rpm for 5 min at 4°C, and a Fyn antibody (20 μL) was added to the supernatant fraction and gently rocked overnight at 4°C. These tubes were centrifuged, and pellets were washed twice. The pellets were suspended in 6.5 μL of kinase buffer supplemented with 10 μL of diluted [γ-^{32}P]ATP solution and 2.5 μL of Src substrate peptide (250 μmol/L) and incubated for 30 min at 30°C.

For the *in vivo* Fyn immunoprecipitation and kinase assay, mice were treated with myricetin (0, 5, 25, or 125 nmol) in 200 μL acetone and dorsal skin prepared as for *in vivo* Western blotting. Proteins were extracted as above and centrifuged at 14,000 rpm for 15 min. In advance, 700 μg of mouse skin extract were mixed with protein-A/G beads (20 μL) for 1 h at 4°C. The mixture was processed, and radioactive incorporation was determined as for the *ex vivo* assay described above. Data are presented as the mean of data points from five mice in each group.

Preparation of myricetin-sepharose 4B. Myricetin-sepharose 4B freeze-dried powder (0.3 g) was suspended in 1 mmol/L HCl and the coupled solution [0.1 mol/L $NaHCO_3$ (pH 8.3) and 0.5 mol/L NaCl] was mixed and rotated at 4°C overnight. The medium was transferred to 0.1 mol/L Tris-HCl buffer (pH 8.0) and again rotated end over end at 4°C overnight. The medium was washed thrice with 0.1 mol/L acetate buffer (pH 4.0) containing 0.5 mol/L NaCl followed by a wash with 0.1 mol/L Tris-HCl (pH 8.0) containing 0.5 mol/L NaCl.

Pull-down assays. For the *ex vivo* pull-down assay, a cellular supernatant fraction of JB6 P+ cells (500 μg) was incubated with myricetin-sepharose 4B (or sepharose 4B alone as a control) beads (100 μL, 50% slurry) in reaction buffer [50 mmol/L Tris (pH 7.5), 5 mmol/L EDTA, 150 mmol/L NaCl, 1 mmol/L DTT, 0.01% Nonidet P-40, 2 μg/mL bovine serum albumin, 0.02 mmol/L phenylmethylsulfonyl fluoride (PMSF), and 1 μg protease inhibitor mixture]. After incubation with gentle rocking overnight at 4°C, the beads were washed five times with buffer [50 mmol/L Tris (pH 7.5), 5 mmol/L EDTA, 150 mmol/L NaCl, 1 mmol/L DTT, 0.01% Nonidet P-40, and 0.02 mmol/L PMSF] and proteins bound to the beads were analyzed by Western blotting. For the *in vivo* pull-down assay, mice received topical application of 200 μL acetone alone or myricetin (5, 25, and 125 nmol) in 200 μL acetone on their shaved backs 1 h before UVB irradiation. Dorsal skin was prepared as described above for the *in vivo* Western blotting, and proteins were extracted as described above for Fyn immunopreciptation and kinase assays. Then 500 μg of mouse skin extract was incubated with myricetin-sepharose 4B (or sepharose 4B alone as a control) beads (100 μL, 50% slurry) in reaction buffer as described for the *ex vivo* pull-down assay. Beads were incubated and washed, and proteins bound to the beads were analyzed by Western blot as described above.

Mouse skin tumorigenesis analysis. Skin carcinogenesis was induced using a UVB irradiation system in mice. The UVB radiation source (Bio-Link cross-linker; Vilber Lourmat) emitted at wavelengths of 254, 312, and 365 nm, with peak emission at 312 nm. SKH-1 mice were divided into four groups of 15 animals each. In the control mice, the dorsal skin was topically treated with 200 μL acetone only. In the UVB group of mice, the dorsal skin was topically treated with 200 μL acetone 1 h before UVB. The mice in the third and fourth groups received topical application of myricetin (8 or 20 nmol) in 200 μL acetone 1 h before UVB irradiation. The UVB dose was 0.18 J/cm^2 given thrice/wk for 27 wk. The incidence of skin tumors was recorded weekly, and a tumor was defined as an outgrowth of >1 mm in diameter that persisted for 2 weeks or more. Tumor incidence, multiplicity, and volume were recorded every wk until the end of the experiment at the 27th week.

Molecular modeling. Insight II (Accelrys, Inc.) was used for the docking study and structure analysis with the crystal coordinates of the kinase domain of Fyn in a complex with staurosporine (accession code 2DQ7), which is available in the Protein Data Bank.[6]

Statistical analysis. As necessary, data were expressed as means ± SE, and the significant differences were determined using one-way ANOVA. A probability value of $P < 0.05$ was used as the criterion for statistical significance. All analyses were performed using Statistical Analysis Software (SAS, Inc.).

Results

Myricetin inhibits UVB-induced COX-2 expression and AP-1 and NF-κB activation. Previous studies have shown that abnormal induction of COX-2 plays an important role in

[6] http://www.rcsb.org/pdb/

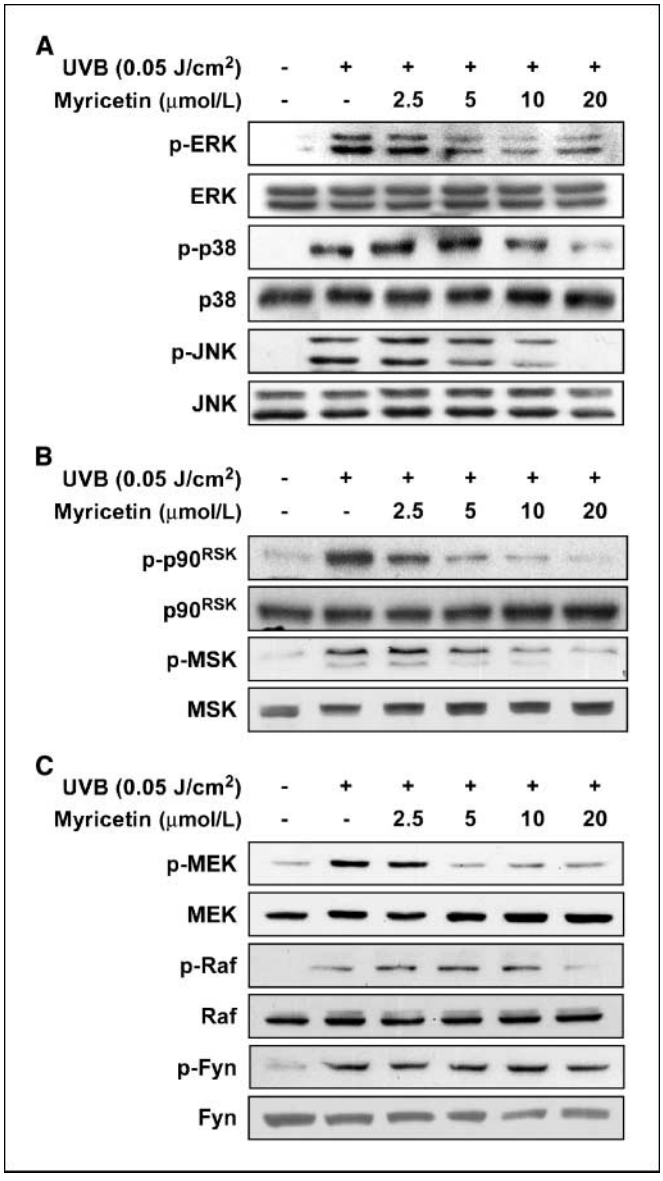

Figure 2. Effects of myricetin on UVB-mediated signaling pathways. *A,* myricetin inhibits UVB-induced phosphorylation (*p-*) of ERK, p38 MAPK, and JNK. *B,* myricetin inhibits UVB-induced phosphorylation of $p90^{RSK}$ and MSK. *C,* myricetin inhibits UVB-induced phosphorylation of MEK and RAF, but not Fyn. Cells were pretreated with myricetin at the indicated concentrations (0, 2.5, 5, 10, or 20 μmol/L) for 1 h, then stimulated with UVB (0.05 J/cm^2), and harvested 15 or 30 min later. The levels of phosphorylated and total ERK, p38 MAPK, JNK, $p90^{RSK}$, MSK, MEK, RAF, and Fyn proteins were determined by Western blot analysis using specific antibodies against the corresponding phosphorylated and total proteins as described in Materials and Methods. Data are representative of three independent experiments that gave similar results.

UV-induced skin cancer (6, 29–31). We first examined the effect of myricetin on UVB-induced COX-2 protein expression and promoter activity using JB6 P+ cells stably transfected with a COX-2–luciferase plasmid. Myricetin inhibited UVB-induced COX-2 protein expression (Fig. 1*B*) and promoter activity in a dose-dependent manner (Fig. 1*C*). Multiple lines of evidence indicate that activation of AP-1 and NF-κB are induced by UV and subsequently induce COX-2 expression and mediate skin cancer (6, 10). Pretreatment of cells with myricetin significantly reduced UVB-induced transactivation of AP-1 or NF-κB in JB6 P+ cells stably transfected with an AP-1–luciferase or an NF-κB–luciferase plasmid (Fig. 1*D*). Myricetin therefore might regulate COX-2 promoter activity and protein expression by suppressing AP-1 and NF-κB activities.

Myricetin suppresses UVB-induced phosphorylation of p38 MAPK, JNKs, and ERKs in JB6 P+ cells. MAPKs, including p38 MAPK, JNKs, and ERKs mediate the up-regulation of AP-1 and NF-κB activity (6, 29, 30). Pretreatment of JB6 P+ cells with myricetin markedly inhibited UVB (0.05 J/cm^2)–induced phosphorylation of p38 MAPK, JNKs, and ERKs (Fig. 2*A*) and also reduced UVB-induced phosphorylation of $p90^{RSK}$ and MSK (Fig. 2*B*), which are downstream of MAPKs. Recent studies have shown that phosphorylation of MAPKs and Src kinase is strongly related to the development of cancer (32). In particular, the Fyn/ERK pathway has been reported to regulate hyperkeratosis and skin cancer (21, 22). Therefore, we examined the effect of myricetin on the UVB-induced Fyn-RAF-MEK signaling pathway. UVB irradiation–induced up-regulation of RAF-MEK phosphorylation was significantly suppressed by myricetin. However, myricetin had no effect on UVB-induced phosphorylation of Fyn (Fig. 2*C*).

Myricetin inhibits Fyn kinase activity by competitively binding with ATP. Because myricetin strongly blocked the UVB-induced phosphorylation of MAPKs, we hypothesized that, although myricetin did not affect UVB-induced phosphorylation of Fyn, it might still directly inhibit Fyn kinase activity. *In vitro* kinase assay data indicated that Fyn kinase activity was substantially induced by UVB (Fig. 3*A*) and was significantly inhibited in a dose-dependent manner by treatment with myricetin (Fig. 3*B*). The time response study showed that Fyn kinase activity in JB6 P+ cells peaked at 10 min after irradiation with UVB (0.05 J/cm^2). The UVB condition [10 min and UVB (0.05 J/cm^2)] was used in an additional study using cell lysates, which revealed that the 6-fold increase in Fyn kinase activity was considerably suppressed by pretreatment with myricetin *ex vivo* (Fig. 3*C*). Because myricetin inhibits Fyn kinase activity, we performed *in vitro* and *ex vivo* pull-down assays to determine whether myricetin interacts directly with Fyn. Results indicated that Fyn was bound with the myricetin-sepharose 4B beads (Fig. 3*D, top, lane 3*), but did not bind with the sepharose 4B beads alone (Fig. 3*D, top, lane 2*). We also observed *ex vivo* binding of myricetin and Fyn in JB6 P+ cell lysates (Fig. 3*D, bottom*), indicating that myricetin directly binds with Fyn. The binding ability of myricetin with Fyn was altered in a concentration-dependent manner in the presence of ATP (Fig. 3*D, bottom, lanes 3–5*), suggesting that myricetin competes with ATP for binding with Fyn. These results suggest that myricetin is an ATP-competitive inhibitor for suppressing Fyn kinase activity.

Myricetin suppresses UVB-induced Fyn kinase activity, COX-2 expression, and phosphorylation of ERK, p38 MAPK, and JNK *in vivo*. Many studies have shown that the rodent model is optimal for studying the mechanisms of skin carcinogenesis (30, 33, 34). We next investigated the effect of myricetin on UVB-induced Fyn kinase activity, COX-2 expression, and phosphorylation of MAPKs using mouse skin. Topical pretreatment with myricetin suppressed UVB-induced Fyn kinase activity in mouse dorsal skin extracts (Fig. 4*A*). We also found that Fyn from these extracts bound to myricetin-sepharose 4B beads (Fig. 4*B, lane 3*), but not to sepharose 4B beads alone (Fig. 4*B, lane 2*). These results suggest that myricetin significantly inhibited Fyn kinase activity by directly binding with Fyn kinase in mouse skin extracts. Further *in vivo* studies showed that topical treatment of myricetin significantly suppressed UVB-induced COX-2 protein expression (Fig. 4*C*) and markedly inhibited phosphorylation of ERKs, p38 MAPK, and

JNKs in mouse skin (Fig. 4*D*). These results clearly showed that UVB-induced Fyn kinase activity was significantly suppressed by topically applied myricetin and that its inhibitory effect is attributable to its regulation of Fyn kinase activity in mouse skin.

Myricetin inhibits UVB-induced skin tumorigenesis in an SKH-1 hairless mouse model. To further study the antitumorigenic activity of myricetin *in vivo*, we evaluated the effect of myricetin in the two-stage UVB-induced skin tumorigenesis model (33, 34). Photographic data show that myricetin inhibited UVB-induced mouse skin cancer development compared with the UVB-only irradiated mice (Fig. 5*A*). Topically applied myricetin (8 or 20 nmol) on mouse skin resulted in a significant inhibition of tumor incidence of 67.4% and 81.7%, respectively ($P < 0.001$ versus the UVB irradiation group, $n = 15$; Fig. 5*B*). The volume of tumors developed in UVB-treated mouse skin was significantly attenuated by myricetin treatment (Fig. 5*C*). Furthermore, the levels of COX-2 expression in the myricetin-treated UVB groups were much lower than COX-2 levels in the UVB-only group (Fig. 5*D*). Overall, these results indicate that myricetin might serve as an effective chemopreventive agent against UVB-mediated skin cancer.

Discussion

A previous study showed that myricetin is a potent inhibitor of bay-region diol-epoxides of polycyclin aromatic hydrocarbon adduct formation in the epidermis and lung of SENCAR mice (35). Myricetin was reported to reduce tumor formation using 7,12-dimethylbenz(*a*)anthracene, benzo(*a*)pyrene, or *N*-methyl-*N*-nitrosoureas initiation and promotion in a skin tumorigenesis model (36). We have shown previously that myricetin strongly

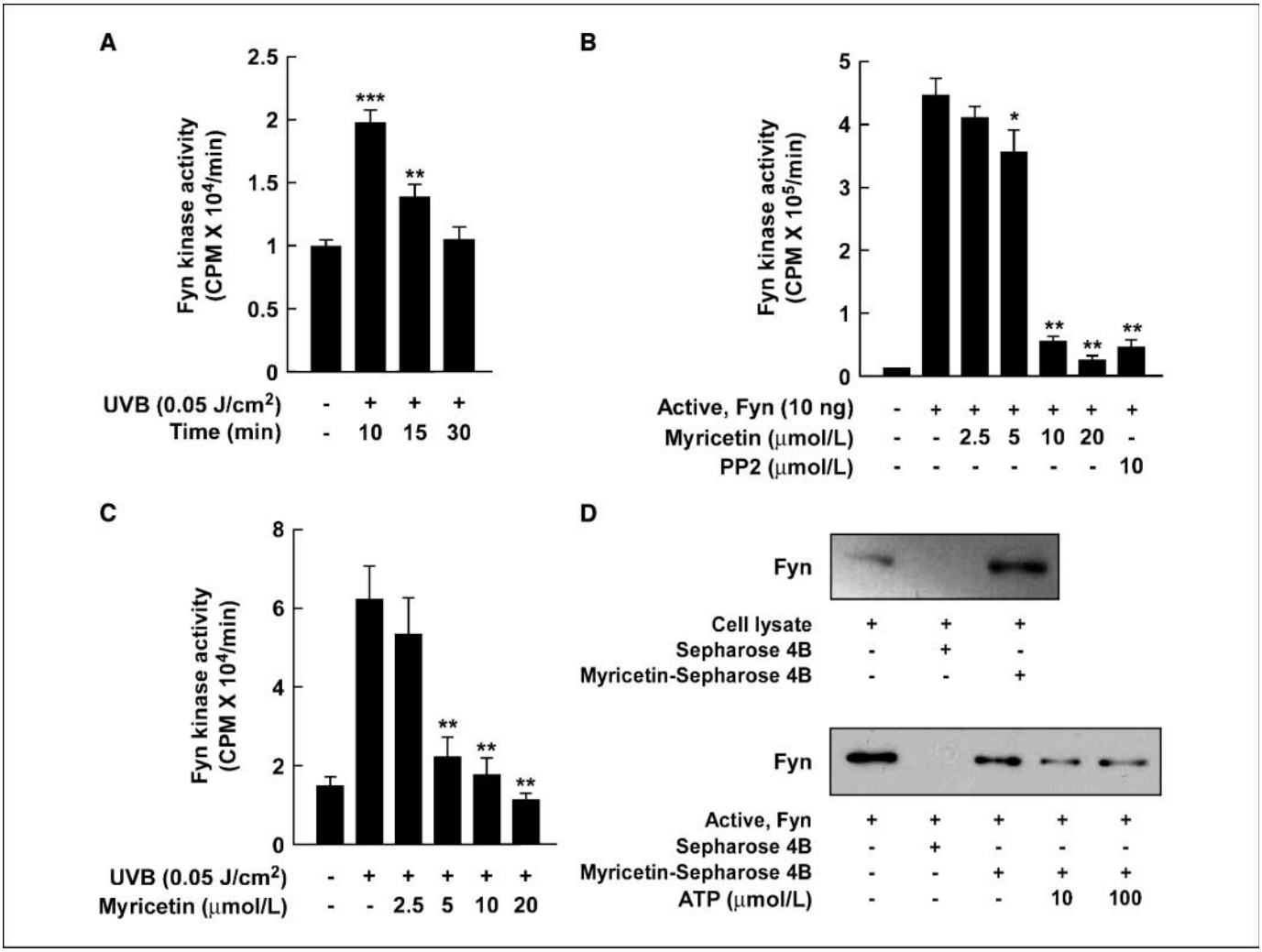

Figure 3. Effects of myricetin on UVB-induced Fyn kinase activity and binding activity. *A,* UVB induces Fyn kinase activity in a time-dependent manner. Myricetin inhibits Fyn kinase activity both *in vitro* (*B*) and *ex vivo* (*C*). The cells were pretreated with myricetin at the indicated concentrations for 1 h and then stimulated with UVB (0.05 J/cm^2) for 15 min. Cells were harvested, and immunoprecipitation and Fyn kinase assays were performed as described in Materials and Methods. *Columns,* mean as determined from three independent experiments; *bars,* SD. *, **, and ***, significant differences at $P < 0.05$, $P < 0.01$, and $P < 0.001$, respectively, between groups treated with UVB and myricetin and the group exposed to UVB alone. *D,* myricetin directly binds with Fyn in an ATP-competitive manner. *Top,* the *ex vivo* myricetin binding was confirmed by immunoblotting using an antibody against Fyn. *Lane 1* (input control), whole-cell lysate from JB6 P+ cells; *lane 2* (control), a lysate of JB6 P+ cells precipitated with sepharose 4B beads as described in Materials and Methods; *lane 3,* whole-cell lysate from JB6 P+ cells precipitated by myricetin-sepharose 4B affinity beads. *Bottom,* active Fyn (2 μg) was incubated with ATP at different concentrations (10 or 100 μmol/L) and 50 μL of myricetin-sepharose 4B or 50 μL of sepharose 4B (as a negative control) in reaction buffer in a final volume of 500 μL. The mixtures were incubated at 4°C overnight with shaking. After washing, the pulled-down proteins were analyzed by Western blot. *Lane 2,* negative control, Fyn cannot bind with Sepharose 4B; *lane 3,* positive control, Fyn binds with myricetin-Sepharose 4B; *lanes 4* and *5,* increasing amounts of ATP suppressed myricetin binding with Fyn. Each experiment was performed thrice.

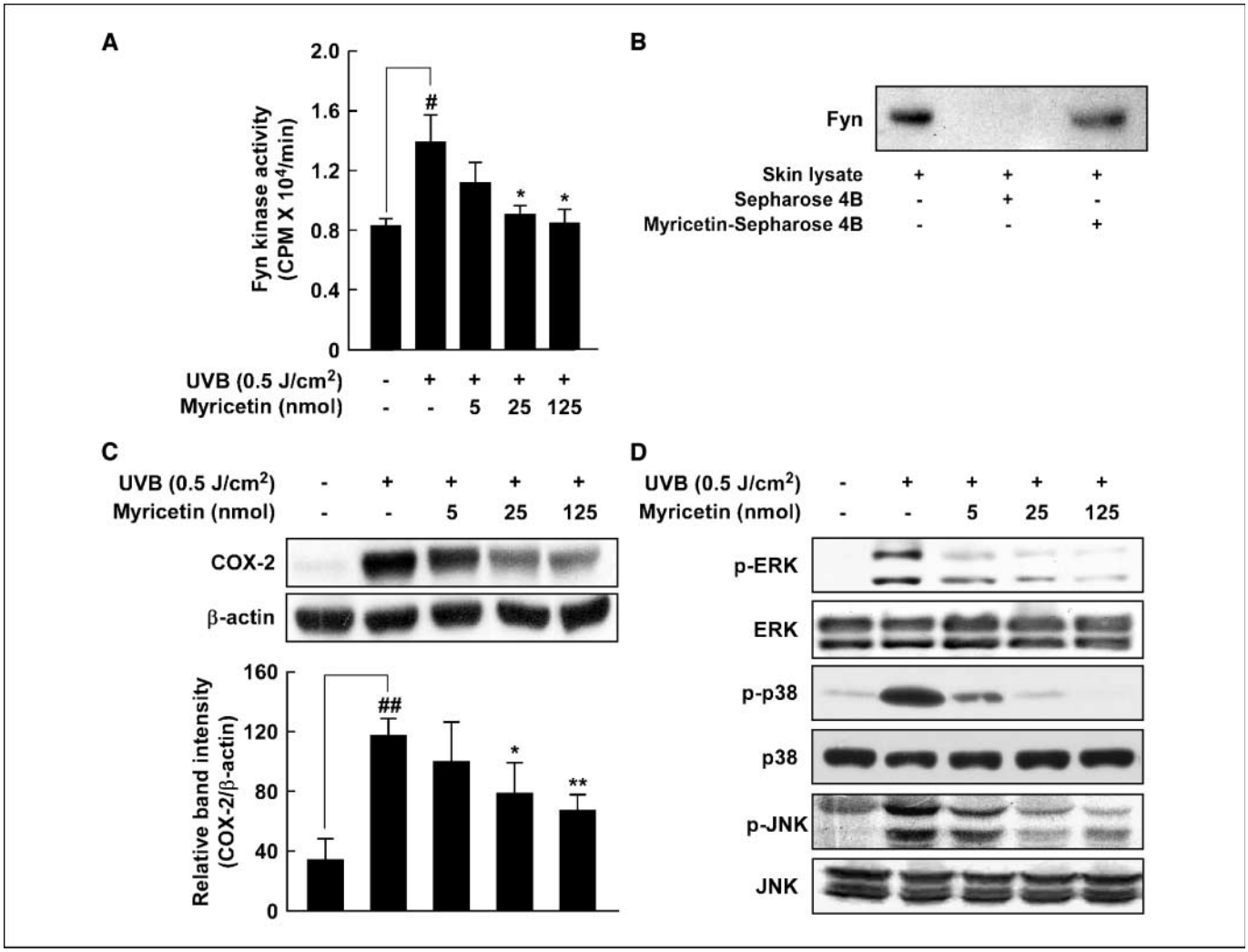

Figure 4. *In vivo* study for the effects of myricetin on UVB-induced Fyn kinase activity, COX-2 expression, and phosphorylation of ERK, p38 MAPK, and JNK in mouse dorsal skin. *A,* myricetin inhibits UVB-induced Fyn kinase activity in mouse skin extracts. For the Fyn kinase assay, dorsal skin protein lysates were prepared from the epidermis, and the assays were carried out as described in Materials and Methods. Each band was quantified by densitometry. *Columns,* mean ($n = 5$); *bars,* SE. #, significant difference ($P < 0.05$) between the control group and the group exposed to UVB (0.5 J/cm^2) alone; *, significant difference ($P < 0.05$) between groups treated with UVB and myricetin and the group exposed to UVB alone. *B,* myricetin specifically binds with Fyn in mouse skin extracts. The Fyn-myricetin binding *in vivo* was confirmed by immunoblotting using an antibody against Fyn; *lane 1* (input control), mouse dorsal skin lysate; *lane 2* (control), a lysate of mouse dorsal skin precipitated with sepharose 4B beads as described in Materials and Methods; *lane 3,* mouse dorsal skin lysate precipitated by myricetin-sepharose 4B affinity beads. Each experiment was performed thrice. *C,* myricetin significantly inhibits UVB-induced COX-2 expression in mouse skin extracts. The levels of COX-2 and β-actin were determined by Western blot analysis using specific antibodies against the corresponding COX-2 and β-actin. Each band was quantified by densitometry. *Columns,* mean ($n = 5$); *bars,* SE. ##, significant difference ($P < 0.01$) between the control group and the group exposed to UVB alone; * and **, significant difference at $P < 0.05$ and $P < 0.05$, respectively, between groups treated with myricetin and irradiated with UVB and the group exposed to UVB alone. *D,* myricetin inhibits phosphorylation of ERK, p38 MAPK, and JNK in mouse skin extracts. The levels of phosphorylated and total ERK, p38 MAPK, and JNK were determined by Western blot analysis using specific antibodies against the corresponding phosphorylated and total proteins. Data are representative of three independent experiments with similar results ($n = 5$).

inhibits 12-*O*-tetradecanoylphorbol-13-acetate or epidermal growth factor (EGF)–induced cell transformation by directly inhibiting MEK activity (28). In the present study, we showed the chemopreventive effect of myricetin on UVB-induced skin cancer and identified molecular mechanism(s) and target(s). COX-2 is induced by cytokines and tumor promoters, and aberrant COX-2 expression has been detected in many human malignancies, including skin cancer. Selective COX-2 inhibitors are known to possess protective effects against UVB-mediated skin cancer. AP-1 and NF-κB are transcription factors that are extremely important in biological events, such as cell proliferation, inflammation, metastasis, and cell transformation (30, 31). Many studies have shown that AP-1 and NF-κB are activated by various tumor promoters and are ideal targets for chemopreventive agents in various cancers, including skin cancer (30). An *in vivo* mouse skin model indicated that AP-1 and NF-κB transactivation plays a critical role in tumor promotion (37). The promoter region of the *Cox-2* gene has binding sites for various transcription factors, including AP-1 and NF-κB (6, 38). We performed a luciferase assay to detect *Cox-2* promoter activity and AP-1 or NF-κB transcription activity. Our results showed that myricetin inhibits COX-2 expression by regulating *Cox-2* promoter activity, which was associated with the inhibition of AP-1 and NF-κB transcription activation. Together, these results suggested that inhibition of UVB-induced COX-2 expression by myricetin

might be at least partially due to an inhibition of AP-1 and NF-κB transactivation.

Previous studies indicated that MAPKs are key molecules activated in response to UVB irradiation and play a critical role in the transcriptional activation of AP-1 and NF-κB (31, 38). Therefore, we determined whether the suppression of MAPK phosphorylation by myricetin could attenuate UVB-stimulated COX-2 expression through the inhibition of AP-1 or NF-κB transcription activity. These results showed that myricetin inhibited UVB-induced phosphorylation of ERK, p38 MAPK, JNK, $p90^{RSK}$, and MSK. Because myricetin suppressed the activation of MAPK signaling, we hypothesized that the molecular target of myricetin to inhibit UVB-induced COX-2 expression might be an upstream kinase of MAPKs. Increased SFK activity is related to many human cancers, including ulcerative colitis, colonic adenocarcinoma, mammary carcinoma, and murine cutaneous squamous cell carcinoma (12–15). A recent report revealed that Fyn regulates UVB-induced phosphorylation of histone H3 and MAPK in JB6 P+ and HaCaT human keratinocytes (39). Based on the above studies and data, we hypothesized that Fyn kinase activity would play a key role in UVB-induced COX-2 expression by regulating MAPKs. Our results clearly showed that myricetin significantly

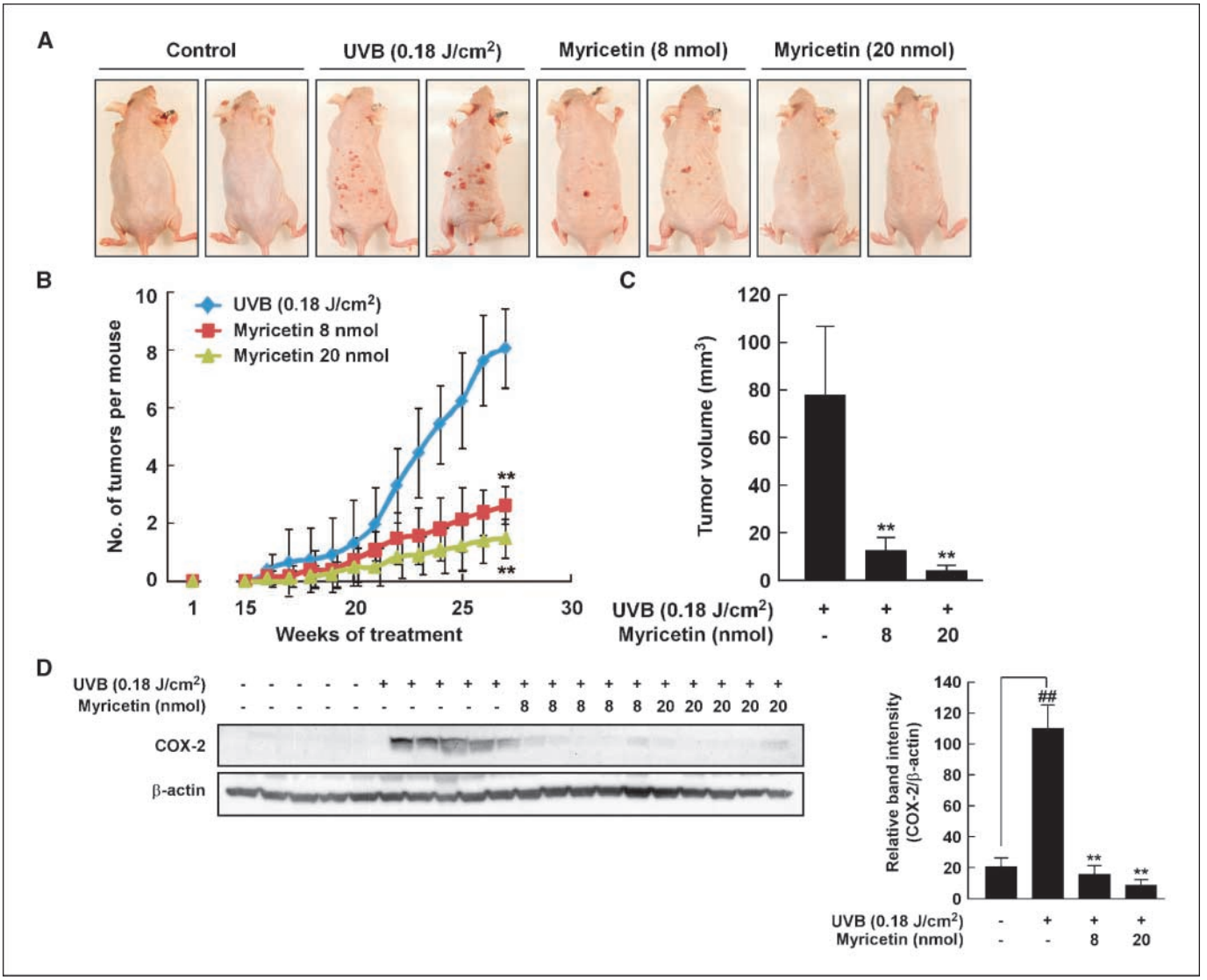

Figure 5. The effect of myricetin on UVB-induced skin carcinogenesis in the SKH-1 hairless mouse. *A,* external appearance of tumors. *B,* myricetin strongly inhibits UVB-induced cancer incidence in the SKH-1 hairless mouse. The control mice (n = 15) received a topical treatment of 200 μL acetone alone (no UVB) and the experimental mice (n = 15) were topically treated with 200 μL acetone before UVB (0.18 J/cm^2) exposure 3 d/wk for 27 wk. The mice in the third and fourth groups received topical application of myricetin (8 or 20 nmol per mouse in 200 μL acetone) on the dorsal surface 1 h before UVB (0.18 J/cm^2) irradiation 3 d/wk for 27 wk. The incidence of skin tumors was recorded weekly, and a tumor was considered to occur when an outgrowth of >1 mm in diameter persisted for 2 wk or longer. Tumor incidence and multiplicity were recorded every week until the end of the experiment at 27 wk. *C,* myricetin strongly suppresses UVB-induced tumor volume in the SKH-1 hairless mouse. The mice were treated as for *B*. At the end of study, the dimension of all tumors on each mouse was recorded. Tumor volumes were calculated using the hemiellipsoid model formula: tumor volume = 1 / 2 (4π / 3) (l / 2) (w / 2) h, wherein l is length, w is width, and h is height. *D,* myricetin strongly inhibits UVB-induced COX-2 expression in the SKH-1 hairless mouse. Skin samples from mice were analyzed for COX-2 expression by immunoblotting. Quantification of COX-2 immunoblot results was normalized to β-actin followed by statistical analysis of relative image density. ##, significant difference (P < 0.01) between the control group and the group exposed to UVB alone; **, significant difference at P < 0.05 between groups treated with myricetin and irradiated with UVB and the group exposed to UVB alone.

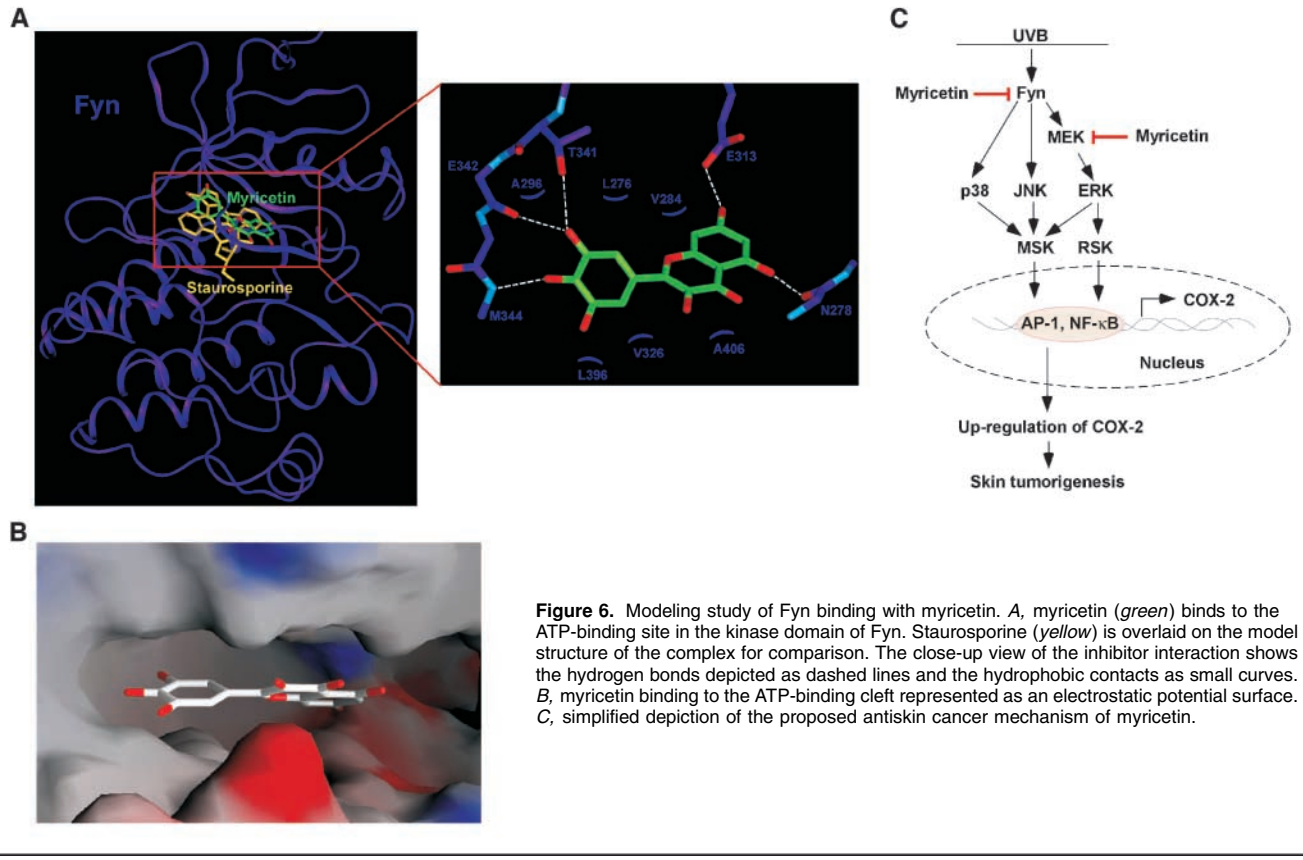

Figure 6. Modeling study of Fyn binding with myricetin. *A,* myricetin (*green*) binds to the ATP-binding site in the kinase domain of Fyn. Staurosporine (*yellow*) is overlaid on the model structure of the complex for comparison. The close-up view of the inhibitor interaction shows the hydrogen bonds depicted as dashed lines and the hydrophobic contacts as small curves. *B,* myricetin binding to the ATP-binding cleft represented as an electrostatic potential surface. *C,* simplified depiction of the proposed antiskin cancer mechanism of myricetin.

inhibited Fyn kinase activity and that the inhibition resulted from ATP-competitive binding of myricetin with Fyn. Furthermore, PP2, a well-known pharmacologic inhibitor of Fyn, and small interfering RNA against Fyn inhibited COX-2 expression by blocking phosphorylation of MAPKs.[7] These results indicated that myricetin suppressed UVB-induced COX-2 expression and subsequently attenuated UVB-induced phosphorylation of MAPKs by regulating Fyn kinase activity.

We further showed that myricetin inhibited UVB-induced COX-2 expression in mouse skin. An *in vivo* study also confirmed previous results showing that myricetin suppressed UVB-induced Fyn kinase activity and subsequently attenuated phosphorylation of MAPKs in mouse skin extracts. We found that the inhibitory effect of myricetin on Fyn kinase activity induced the suppression of MAPKs phosphorylation and most likely was due to myricetin specifically binding with Fyn in JB6 P+ cells and mouse skin. In melanoma progression, activation of Fyn leads to melanocyte differentiation by modified MAPK activity (40). Increased epidermal Fyn levels are associated with the activation of ERK, signal transducers and activators of transcription-3 (STAT-3), and PDK-1 in keratin 14-Fyn (K14) transgenic mice (41). A recent study showed that binding between EGCG and Fyn reduced EGF-induced cell transformation and p38 phosphorylation in JB6 P+ cells (42). Previous studies also suggest a relationship between Fyn and various transcription factors, including activating transcription factor-2 (42), STAT (43, 44), and cAMP-responsive element binding protein (38). These results suggest that myricetin inhibits UVB-induced skin carcinogenesis through the inhibition of transcription factors and MAPKs by targeting Fyn.

A modeling study was performed using the crystal structure of the Fyn kinase domain in complex with staurosporine, a well-known kinase inhibitor (45). Myricetin easily docked to the ATP-binding site of Fyn, which is located between the N and C lobes of the kinase domain (Fig. 6*A* and *B*). Myricetin can form hydrogen bonds with the backbone of the hinge region of Fyn, as seen in other ATP-competitive kinase inhibitors. The docking data indicate that myricetin was easily docked to the ATP-binding site of Fyn. Our pull-down assay, which shows that myricetin competes with ATP for binding with Fyn, supports the docking results. The hydroxyl group at the 4′ position works as a hydrogen bonding acceptor in the interaction with the backbone amide group of Met^{344}, and the hydroxyl group at the 3′ position is a hydrogen bonding donor in the interaction with the backbone carbonyl group of Glu^{342}. At the same time, it can also work as a hydrogen bonding acceptor to interact with the side chain of Thr^{341}. The hydroxyl group at the 7 position would make a hydrogen bond with the side chain of Glu^{313} and the hydroxyl group at the 5 position could also form a hydrogen bond with the backbone carbonyl group of Asn^{278}. In addition, the inhibitor would be sandwiched by hydrophobic residues, including Leu^{276}, Val^{284}, and Ala^{296} from the N-lobe and Val^{326}, Leu^{396}, and Ala^{406} from the C-lobe, and thereby lead to the high activity of the inhibitor for Fyn. Further studies with X-ray crystallography to determine the inhibitor complex structure would elucidate the exact binding mode of myricetin and Fyn.

[7] Unpublished observation.

Clinical observations and epidemiologic data strongly suggest that nonmelanoma skin cancer is related to chronic exposure to UV (4, 6, 30). Our results clearly showed that topical application of myricetin markedly inhibits the formation of skin cancer in the SKH-1 hairless mouse model. This inhibition occurs mainly through the blocking of Fyn, suggesting that Fyn is a critical target for myricetin in mediating COX-2 expression through the inhibition of MAPKs via regulation of AP-1 and NF-κB activity. A simplified depiction of our proposed antiskin cancer mechanism of myricetin is shown in Fig. 6*C*. Therapeutic inhibition of Fyn kinase activity by myricetin might provide clinical benefit in skin cancer.

Disclosure of Potential Conflicts of Interest

No potential conflicts of interest were disclosed.

Acknowledgments

Received 3/11/2008; revised 4/24/2008; accepted 4/29/2008.

Grant support: Hormel Foundation, NIH grants CA027502, CA120388, CA111536, CA088961, and CA081064, and BioGreen21 Program grants 20070301-034-027 and 20070301-034-042, Rural Development Administration, Republic of Korea.

The costs of publication of this article were defrayed in part by the payment of page charges. This article must therefore be hereby marked *advertisement* in accordance with 18 U.S.C. Section 1734 solely to indicate this fact.

The University of Minnesota is an equal opportunity educator and employer.

References

1. Melnikova VO, Ananthaswamy HN. Cellular and molecular events leading to the development of skin cancer. Mutation research 2005;571:91–106.
2. Setlow RB. The wavelengths in sunlight effective in producing skin cancer: a theoretical analysis. Proc Natl Acad Sci U S A 1974;71:3363–6.
3. Ley RD. Photoreactivation in humans. Proc Natl Acad Sci U S A 1993;90:4337.
4. Matsumura Y, Ananthaswamy HN. Short-term and long-term cellular and molecular events following UV irradiation of skin: implications for molecular medicine. Exp Rev Mol Med 2002;4:1–22.
5. Matsumura Y, Ananthaswamy HN. Toxic effects of ultraviolet radiation on the skin. Toxicol Applied Pharmacol 2004;195:298–308.
6. Bode AM, Dong Z. Mitogen-activated protein kinase activation in UV-induced signal transduction. Sci STKE 2003;2003:RE2.
7. Smith WL, DeWitt DL, Garavito RM. Cyclooxygenases: structural, cellular, and molecular biology. Ann Rev Biochem 2000;69:145–82.
8. Chen W, Tang Q, Gonzales MS, Bowden GT. Role of p38 MAP kinases and ERK in mediating ultraviolet-B induced cyclooxygenase-2 gene expression in human keratinocytes. Oncogene 2001;20:3921–6.
9. Fischer SM, Lo HH, Gordon GB, et al. Chemopreventive activity of celecoxib, a specific cyclooxygenase-2 inhibitor, and indomethacin against ultraviolet light-induced skin carcinogenesis. Mol Carcinog 1999;25:231–40.
10. Lee JL, Mukhtar H, Bickers DR, Kopelovich L, Athar M. Cyclooxygenases in the skin: pharmacological and toxicological implications. Toxicol Applied Pharmacol 2003;192:294–306.
11. Thomas SM, Brugge JS. Cellular functions regulated by Src family kinases. Ann Rev Cell Dev Biol 1997;13:513–609.
12. Cartwright CA, Coad CA, Egbert BM. Elevated c-Src tyrosine kinase activity in premalignant epithelia of ulcerative colitis. J Clin Investig 1994;93:509–15.
13. Matsumoto T, Jiang J, Kiguchi K, et al. Overexpression of a constitutively active form of c-src in skin epidermis increases sensitivity to tumor promotion by 12-O-tetradecanoylphorbol-13-acetate. Mol Carcinog 2002;33:146–55.
14. Muthuswamy SK, Muller WJ. Activation of Src family kinases in Neu-induced mammary tumors correlates with their association with distinct sets of tyrosine phosphorylated proteins *in vivo*. Oncogene 1995;11:1801–10.
15. Park J, Meisler AI, Cartwright CA. c-Yes tyrosine kinase activity in human colon carcinoma. Oncogene 1993;8:2627–35.
16. Calautti E, Missero C, Stein PL, Ezzell RM, Dotto GP. fyn tyrosine kinase is involved in keratinocyte differentiation control. Genes Dev 1995;9:2279–91.
17. Matsumoto T, Jiang J, Kiguchi K, et al. Targeted expression of c-Src in epidermal basal cells leads to enhanced skin tumor promotion, malignant progression, and metastasis. Cancer Res 2003;63:4819–28.
18. Resh MD. Fyn, a Src family tyrosine kinase. Int J Biochem Cell Biol 1998;30:1159–62.
19. Li X, Yang Y, Hu Y, et al. αvβ6-Fyn signaling promotes oral cancer progression. J Biol Chem 2003;278:41646–53.
20. Calautti E, Grossi M, Mammucari C, et al. Fyn tyrosine kinase is a downstream mediator of Rho/PRK2 function in keratinocyte cell-cell adhesion. J Cell Biol 2002;156:137–48.
21. Ilic D, Kanazawa S, Nishizumi H, et al. Skin abnormality in aged $fyn^{-/-}fak^{+/-}$ mice. Carcinogenesis 1997;18:1473–6.
22. Mariotti A, Kedeshian PA, Dans M, Curatola AM, Gagnoux-Palacios L, Giancotti FG. EGF-R signaling through Fyn kinase disrupts the function of integrin α6β4 at hemidesmosomes: role in epithelial cell migration and carcinoma invasion. J Cell Biol 2001;155:447–58.
23. Surh YJ. Cancer chemoprevention with dietary phytochemicals. Nat Rev 2003;3:768–80.
24. German JB, Walzem RL. The health benefits of wine. Ann Rev Nutr 2000;20:561–93.
25. Hakkinen SH, Karenlampi SO, Heinonen IM, Mykkanen HM, Torronen AR. Content of the flavonols quercetin, myricetin, and kaempferol in 25 edible berries. J Agric Food Chem 1999;47:2274–9.
26. Sellappan S, Akoh CC. Flavonoids and antioxidant capacity of Georgia-grown Vidalia onions. J Agric Food Chem 2002;50:5338–42.
27. Ribeiro de Lima MT, Waffo-Teguo P, Teissedre PL, et al. Determination of stilbenes (trans-astringin, cis- and trans-piceid, and cis- and trans-resveratrol) in Portuguese wines. J Agric Food Chem 1999;47:2666–70.
28. Lee KW, Kang NJ, Rogozin EA, et al. Myricetin is a novel natural inhibitor of neoplastic cell transformation and MEK1. Carcinogenesis 2007;28:1918–27.
29. Karin M. Mitogen-activated protein kinase cascades as regulators of stress responses. Ann N Y Acad Sci 1998;851:139–46.
30. Bode AM, Dong Z. Signal transduction pathways: targets for chemoprevention of skin cancer. Lancet Oncol 2000;1:181–8.
31. Ding M, Feng R, Wang SY, et al. Cyanidin-3-glucoside, a natural product derived from blackberry, exhibits chemopreventive and chemotherapeutic activity. J Biol Chem 2006;281:17359–68.
32. Marshall CJ. Specificity of receptor tyrosine kinase signaling: transient versus sustained extracellular signal-regulated kinase activation. Cell 1995;80:179–85.
33. Mallikarjuna G, Dhanalakshmi S, Singh RP, Agarwal C, Agarwal R. Silibinin protects against photocarcinogenesis via modulation of cell cycle regulators, mitogen-activated protein kinases, and Akt signaling. Cancer Res 2004;64:6349–56.
34. Aziz MH, Reagan-Shaw S, Wu J, Longley BJ, Ahmad N. Chemoprevention of skin cancer by grape constituent resveratrol: relevance to human disease? FASEB J 2005;19:1193–5.
35. Das M, Khan WA, Asokan P, Bickers DR, Mukhtar H. Inhibition of polycyclic aromatic hydrocarbon-DNA adduct formation in epidermis and lungs of SENCAR mice by naturally occurring plant phenols. Cancer Res 1987;47:767–73.
36. Mukhtar H, Das M, Khan WA, Wang ZY, Bik DP, Bickers DR. Exceptional activity of tannic acid among naturally occurring plant phenols in protecting against 7,12-dimethylbenz(a)anthracene-, benzo(a)pyrene-, 3-methylcholanthrene-, and N-methyl-N-nitrosourea-induced skin tumorigenesis in mice. Cancer Res 1988;48:2361–5.
37. Young MR, Li JJ, Rincon M, et al. Transgenic mice demonstrate AP-1 (activator protein-1) transactivation is required for tumor promotion. Proc Natl Acad Sci U S A 1999;96:9827–32.
38. Bowden GT. Prevention of non-melanoma skin cancer by targeting ultraviolet-B-light signalling. Nat Rev 2004;4:23–35.
39. He Z, Cho YY, Ma WY, Choi HS, Bode AM, Dong Z. Regulation of ultraviolet B-induced phosphorylation of histone H3 at serine 10 by Fyn kinase. J Biol Chem 2005;280:2446–54.
40. Wellbrock C, Weisser C, Geissinger E, Troppmair J, Schartl M. Activation of p59(Fyn) leads to melanocyte dedifferentiation by influencing MKP-1-regulated mitogen-activated protein kinase signaling. J Biol Chem 2002;277:6443–54.
41. Li W, Marshall C, Mei L, Gelfand J, Seykora JT. Srcasm corrects Fyn-induced epidermal hyperplasia by kinase down-regulation. J Biol Chem 2007;282:1161–9.
42. He Z, Tang F, Ermakova S, et al. Fyn is a novel target of (-)-epigallocatechin gallate in the inhibition of JB6 Cl41 cell transformation. Mol Carcinog 2008;47:172–83.
43. Zhang Y, Liu G, Dong Z. MSK1 and JNKs mediate phosphorylation of STAT3 in UVA-irradiated mouse epidermal JB6 cells. J Biol Chem 2001;276:42534–42.
44. Li W, Marshall C, Mei L, et al. Srcasm modulates EGF and Src-kinase signaling in keratinocytes. J Biol Chem 2005;280:6036–46.
45. Kinoshita T, Matsubara M, Ishiguro H, Okita K, Tada T. Structure of human Fyn kinase domain complexed with staurosporine. Biochem Biophys Res Commun 2006;346:840–4.